Computer Modeling for Stabilities and Structural Relationships of n-Hydrocarbons

J.W. HAGEMANN and **J.A. ROTHFUS**, Northern Regional Research Center, Federal Research, Science and Education Administration, U.S. Department of Agriculture,[1] Peoria, Illinois 61604

ABSTRACT

Atom-atom spatial interactions were calculated for the four crystal packings known to exist in n-alkanes. Expression of end-group or mid-chain interactions as fractions of overall intermolecular interactions did not require use of the classical sixth power Lennard-Jones potential, yet allowed estimation of melting points within a given structural series and accurate prediction of the melting point of polyethylene. The calculations also provide a basis for explanation of structural relationships and stabilities among the four different n-paraffin forms.

INTRODUCTION

Earlier work (1) on the thermal behavior of single acid triglycerides found new melting forms that are yet unconfirmed by alternative procedures. X-ray studies might provide the most direct confirmation of these new forms, but instabilities of the polymorphs in question and the difficulty of growing single crystals have compelled exploration of other alternatives. Conformational analysis by computer modeling, which can provide comparative information not dependent on stability or availability of sample, is an especially promising technique. We modeled n-alkane chain segments preparatory to analysis of triglyceride structures and have found the method useful in projecting properties and accounting for structural relationships and stabilities.

Depending on temperature and pressure, linear hydrocarbon chains adopt crystal structures that are hexagonal, H(2); orthorhombic $0_\perp$ (3); monoclinic, M (2); or triclinic, T// (4). These four types of chain packing are illustrated schematically in Figure 1. Each form of packing can be converted to the other forms by chain reorientation if chain tilt is disregarded. Orthorhombic crystals, in which the zigzag chains are perpendicular to end-group planes, thus share the same subcell configuration with monoclinic crystals, in which chains intersect end-group planes at an angle. Chain tilt cannot be neglected, however, since it introduces packing efficiencies and stabilization that further contribute significantly to the thermal behavior of crystalline alkanes.

Using the traditional symbols α and β to designate high and low temperature phases (5), crystalline n-alkane structures are thus referred to as α_H, β_O, β_M, and β_T. The α_H and β_O structures have chains that are vertical to end group planes, whereas β_M and β_T chains are tilted. The crystalline structures of the normal alkanes have been covered adequately in a review by Turner (6). Briefly, the α_H form of alkanes is the one which odd alkanes from C_9-C_{43} and even alkanes from C_{22}-C_{42} first assume on cooling from the melt. The β_O form is the stable phase of odd normal alkanes C_9 and above and perhaps all even alkanes above C_{30} or C_{32}. When even alkanes C_{24} or C_{26} and above are cooled from the α_H or β_O phases, the β_M form is attained; even alkanes from about C_8-C_{26} enter the β_T phase upon cooling either from the melt or α_H form. Thus it can be said that while β_O and β_T predominate in shorter odd and even alkanes, longer chain length alkanes, both odd and even, can exist in either the β_O or β_M structures.

Whereas hydrocarbon chains are constituents of all different types of lipid structures, an understanding of the information attainable from n-alkane models and simple means of deriving such information are required to extend these same techniques to prediction of structures and properties for larger lipid molecules.

EXPERIMENTAL

A space-filling model was constructed by programming the x-, y-, and z-axis coordinates for each carbon atom of

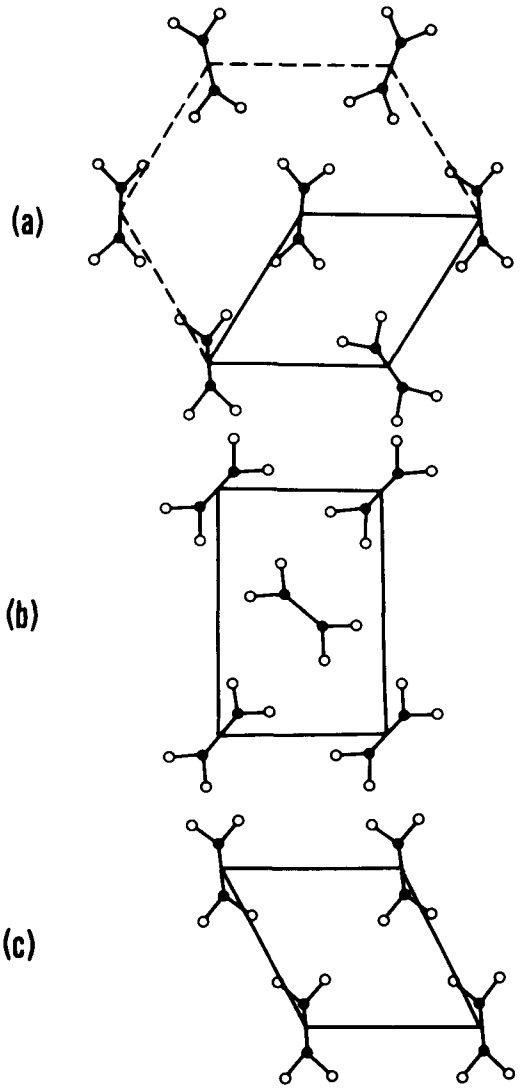

FIG. 1. Types of n-alkane subcell packing shown projected on cross sections perpendicular to the chain axes. Solid circles indicate carbon atoms and open circles are hydrogen atoms. (a) hexagonal in α_H; (b) orthorhombic, vertical chains in β_O, tilted chains in β_M; (c) triclinic in β_T.

[1]The mention of firm names or trade products does not imply that they are endorsed or recommended by the U.S. Department of Agriculture over other firms or similar products not mentioned.

two groups of zigzag alkane chaines, each consisting of 180 carbon atoms, into an IBM 1130 computer using Fortran IV language according to the diagram of Figure 2a. One group of chains was situated directly above the other; each consisted of three rows having three 20-carbon segments. Carbon atoms were numbered with the lower block of atoms numbered 1-180 and the upper block numbered 181-360. Two hydrogen atoms were placed on all the 360 carbon atoms, and each terminal carbon carried an additional hydrogen to properly simulate structure at the methyl gap between chains. The three coordinates of each of the 360 carbon atoms were put in computer memory, but coordinates for the hydrogen atoms were calculated during computation because of the limited computer core.

Subcell dimensions used for each type structure are given in Table I. Programs were written so chains could be twisted or rows offset according to Figure 2b, or could be lifted along the x- or y-axis (Fig. 2c) to produce various angles of tilt at the methyl gap. Programming for angle of tilt was simplified by the fact that chains could be arranged vertically with respect to the xy axis, and adjacent chains in each row could be lifted by multiples of the c_s dimension.

Specific subcell conformations were simulated by adjusting the matrixed chains to fit selected subcell dimensions. For example, offsetting the center row of chains in Figure 2a to the right, as in Figure 2b, until chain 61-80 is midway between chains 1-20 and 21-40 produces the general subcell pattern for H and $0_\perp$. Adding chain twist, random for H or parallel in alternate rows for $0_\perp$, finalizes these subcell structures. Slightly less offset with parallel zig-zag planes produces the T// structure.

Standard bond lengths and angles for carbon and hydrogen and Van der Waals radii of 1.2 Å for hydrogen and 2.0 Å for methyl groups (7) were used throughout the programs. Subcell dimensions listed in Table I were used except for c_s, where 2.5 Å was applied to all programs.

It was assumed that the same calculations performed on all structures would allow valid comparison of different model perturbations. A potential function and constants reported by Coiro et al. (8) were used to calculate atom-atom interactions that could be expressed in kcal per atom pair when interatomic distances were in angstroms. Only the "attractive" term of this function was needed for our purposes, since the interactions of interest occur outside the limits for significant nuclear repulsion. The repulsive term is less than 10% of the total potential function over most interatomic distances calculated and is significant only between nearest neighbors. The attractive term consists of a constant, which depends on the type of interaction, divided by the sixth power of the interatomic distance (c/r^6). Calculation of all possible interactions, H-H, C-H, and C-C, was performed only for the β_M structure; H-H calculations were sufficient for all other structures. Since approximations were inherent in this method, each result is an estimated interaction (EI). Using a cut-off distance of r=6 Å, the proton EI values range from 0.468 for minimum proton approach of 2.4 Å to 0.00192 for the cut-off distance. Minimum C-C distance in β_M, fixed by the subcell dimensions, was 4.1 Å. For comparison, H-H calculations were also performed on all structures using r^2 instead of r^6.

Sequentially, the program was executed as follows: First, a table listing the coordinates of all 360 carbon atoms and their attached protons (three protons for the terminal carbons at the methyl gap) was generated. Next, the identification of a particular proton on a particular carbon was inserted, and all protons within 6 Å were found and listed in printout along with the distance to each and the EI value. At the end, a total EI was given for the proton in question. In this manner, a sphere of influence around a proton could be determined and readily compared to another proton in a different environment.

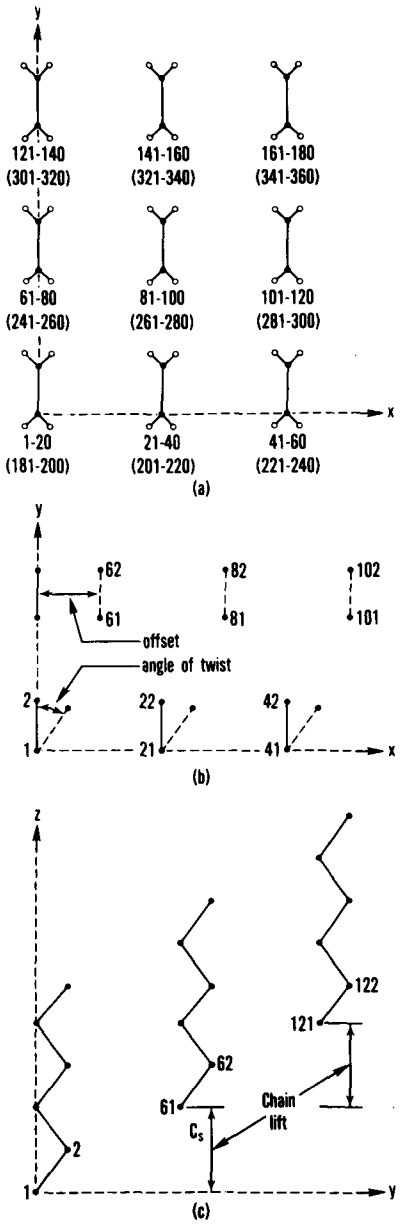

FIG. 2. (a) Arrangement and numbering of carbon atoms in computer modeling program. Solid circles indicate carbon atoms and open circles are hydrogen atoms. Numbers in parenthesis refer to upper block of carbon atoms. (b) Methods used to vary arrangements of carbon atoms to produce different subcell packings. Hydrogen atoms are not indicated. (c) Method used to produce tilted chains. Hydrogen atoms are not indicated.

Calculations were generally done on atoms in chains 81-100 or 261-280 (Fig. 2a) as these chains were completely surrounded by adjacent chains. EIs were not calculated between atoms in the chain containing the atom used to define a sphere of influence. Proton EIs were determined for all carbons from about the middle of the chain to the methyl protons, thereby showing changes taking place in protons near and at the methyl gap. This was likewise done for all C-H and C-C calculations. Interactions within 6 Å but across the methyl gap were also recorded in the output listing.

The correctness of the various arrays was determined by checking the three coordinates of the carbon atoms with the angles and subcell dimensions listed in the program. Also, stereochemistry and programming were assumed to be correct, if similar EIs were found for comparable atoms in both groups of chains.

TABLE I

Dimensions of n-Alkane Chain Subcells

Structure type	Symbol	a_s (Å)	b_s (Å)	c_s (Å)	Volume/CH_2 (Å^3)	Ref.
Hexagonal	H	4.9	—	2.5	26.0	2
Orthorhombic	$O_\perp$	4.90	7.41	2.54	23.1	3
Triclinic	T//	4.41	5.40	2.45	23.7	4

TABLE II

Estimated Interactions in kcal of Protons in Alkane Subcell Packings (Total Number of Interactions in Parentheses)

Hydrocarbon type	Structure type	Middle of chain	6th Carbon protons	5th Carbon protons	4th Carbon protons	3rd Carbon protons	2nd Carbon protons	CH_3 Protons
α_H	H	2.472 (67)	2.472 (67)	2.472 (67)	1.975 (65)	2.445 (67)	1.889 (61)	2.682 (101)
β_T	T//	2.360 (112)	2.362 (113)	2.360 (112)	2.332 (106)	2.340 (105)	1.834 (104)	3.209 (159)
β_O	$O_\perp$ vertical	3.581 (120)	3.581 (120)	3.581 (120)	3.574 (123)	3.548 (114)	3.466 (110)	3.869 (178)
β_M	$O_\perp$ tilted	3.583 (120)	3.583 (120)	3.569 (118)	3.558 (121)	3.138 (111)	3.271 (119)	3.769 (179)

The EIs reported for the hexagonal structure, which has chains of random twist, are the average of two different arrangements for both the lower and upper groups of carbons. Although a compromise, this average still allowed comparison of the H structure with other more ordered forms.

RESULTS

H-H interaction data for the four crystal structures are given in Table II. The EIs listed for particular carbon atoms are the sum of the total EI for each of the two protons (three for the methyl group). Numbers in parentheses refer to the total number of interactions found within 6 Å from the two or three protons. It should be noted that for α_H and β_O, EIs of protons on the 5th and 6th carbons from the end of the chain are the same as the EI for protons in the middle of the chain, which—for our purposes—began with the carbon beyond which computations resulted in the same total EI. Thus, for T//, constant values were not obtained until the 7th carbon from the end was reached. The start of middle-of-chain packing is affected by both the cut-off value of the interatomic distance, r, and the angle of tilt, but the value for r need not be large because many hydrocarbon properties are determined by interactions near the methyl gap (9). Our calculations indicate that methyl group influence on methylene packing rapidly becomes insignificant beyond the 5th or 6th penultimate carbon even though substantial differences in methyl group interaction are apparent between the four crystal types. Orthorhombic structures have the highest methyl and mid-chain interactions of the subcell arrangements; H have the lowest. This is in agreement with the volume/CH_2 group (Table I) which shows the orthorhombic to have the most dense packing and H the least.

EIs for 2nd carbon protons (Table II) are somewhat lower than for the other carbon positions, especially in α_H and β_T. For this carbon, a considerable portion of the 6 Å distance not only ends in the methyl gap region but also extends to protons across the methyl gap near the 6 Å limit. Although the number of interactions is about the same for each type structure, many of the values are near the lower limit. With more dense packing, $O_\perp$ structures, the effect is not as large. Tilting of chains also reduces the interaction, β_O vs. β_M, by moving some protons away from the methyl gap.

Middle-of-Chain Interactions

EIs of entire hydrocarbon chains were determined for a number of chain lengths using the structure-type data in Table II. Total molecule EIs were calculated by adding together the number of particular proton EIs present in the molecule. For example, a T// structure of C_{14} would have two each of CH_3 to 6th carbon protons groups plus two middle-of-chain groups. End group influence was separated from that of the middle of the chain by calculating a ratio (REI) of the total middle-of-chain interaction over the total interaction for the whole molecule. Listed in Table III are the REIs determined for several alkanes from C_{26} to C_{44} for the three types of interactions in the β_M structure. Although the values change systematically with chain length, the data (Table III) indicate that the contribution of the middle of the chain, or conversely the end groups, is essentially independent of the type of interaction. The C-C ratio was the highest of the three, but only about 5% higher than H-H at C_{26}, and decreases with increased chain length. When all three interactions are combined, the REI is very similar to any one of the three and closely approximates the average. Even though r^2 data represent a much smaller part of the total energy curve than do r^6 data, when expressed as a ratio very little difference is found. Comparing the H-H REI results, the r^2 data are less than 1% lower than the r^6 data. These results suggest that for hydrocarbon type molecules, when data are expressed as ratios, no additional information is gained from the C-H and C-C results nor from the classical r^6 potential function (10).

Melting Points

Plots were made (Fig. 3) of REI vs. melting point (5, 11-13) for hydrocarbons in β_T, β_O, and β_M structures. Computer results were obtained using the subcell structure normally assigned to the particular chain length. For each of the three structures, a parabolic curve gave a better fit than the least squares line and had standard errors of 0.2 K

TABLE III

Ratio of the Middle-of-Chain Interaction to Total Interaction for β_M

Hydrocarbon chain length	REI[a] H-H	C-H	C-C	Total REI[b]	H-H REI for r^2 data
26	0.610	0.632	0.643	0.625	0.605
30	0.662	0.682	0.692	0.676	0.656
34	0.701	0.720	0.730	0.714	0.696
38	0.733	0.750	0.759	0.745	0.728
44	0.769	0.785	0.793	0.780	0.765

[a]REI = Ratio of estimated interactions.
[b]Combined H-H, C-H, and C-C data.

for β_T (C_{14}-C_{28}), 0.6 for β_O (C_{11}-C_{67}) and 0.3 for β_M (C_{26}-C_{100}). Calculations were performed for the chain length ranges indicated but were recorded to only C_{43} in Figure 3. Standard errors for the least squares lines were 0.8 (β_T), 2.8 (β_O), and 1.0 (β_M).

Heats of Fusion

Plots of ΔH_f values of n-alkanes (11,12) vs. computer results gave a good parabolic curve fit for β_T, standard error of 0.1 Kcal/mol; but relationships for β_O and β_M were not as good, with standard errors of 0.8 for both. This was primarily due to the fact that ΔH_f values above C_{28} are not reported for the same crystalline transition. The following equations were found for the three crystal types.

β_T: ΔH_f (kcal/mol) = 43.51 REI^2 + 0.19 REI + 10.00

β_O: ΔH_f (kcal/mol) = 106.37 REI^2 - 67.72 REI + 18.34

β_M: ΔH_f (kcal/mol) = -165.26 REI^2 + 297.66 REI - 97.73

DISCUSSION

Alkane crystal structures owe their stability to two types of interactions, lateral association of zig-zag chains and interaction across gaps between methyl end-group planes (6). Our results (Table II) indicate that, depending on subcell conformation, stabilizing interactions across the methyl gap can extend 5 to 7 carbons into adjoining layers of chains. Beyond that limit, chain stability derives primarily from middle-of-chain interaction.

In terms of our results, middle-of-chain interaction is ill-defined for alkanes shorter than n-decane. For normal alkanes longer than C_{10}, however, the contribution from methyl to middle-of-chain structure soon becomes a constant, and increasing chain length merely increments the molecular EI by a constant amount equal to the middle-of-chain interaction (Table II).

Molecular EIs, though easily predicted, reflect inadequately the specific balance of lateral and end-group interactions that imparts characteristic thermal properties to each alkane crystal structure. Such information, which is important in projecting polymorphic behavior from knowledge of chemical structure, becomes more obvious when the total middle-of-chain interaction is related to the total molecular interaction via REI.

H-H REI values calculated for C_{10} to C_{28} alkanes in the structure normally assigned to the particular chain length (6) are listed in Table IV. REIs calculated for C_{12} to C_{24} hydrocarbons in the β_M form are also listed for comparison, even though such structures are hypothetical from a practical standpoint.

Chain Length and Stability

One of the more interesting features of normal paraffin behavior with respect to increasing chain length is a sharp change in crystal structure around C_{26} where even length chains change from β_T to β_M (Fig. 3). The theoretical reason for this change is not yet clear though there is a consensus that the shift reflects a diminishing effect of end groups versus chain groups on the enthalpy of the crystal (6). Our calculations support this consensus. In Table IV, the REI of C_{26} for β_T is about 53%, but for β_M, 61%. At this chain length, middle-of-chain and end group energies are nearly the same for β_T. For β_M, however, the middle-of-chain contribution definitely predominates, which would favor conversion to an orthorhomib subcell structure (β_M) rather than maintenance of the β_T form.

This correlation of a sharp change in physical behavior with calculated interaction energies imparts an unanticipated significance to REI values. Curiously, the importance of a 60% middle-of-chain contribution identified by this correlation is borne out through examination of yet another instance of chain length effect on crystal stability. When cooled, normal alkanes longer than C_{20} pass from the liquid into β_T crystals via a stable α_H form that is also

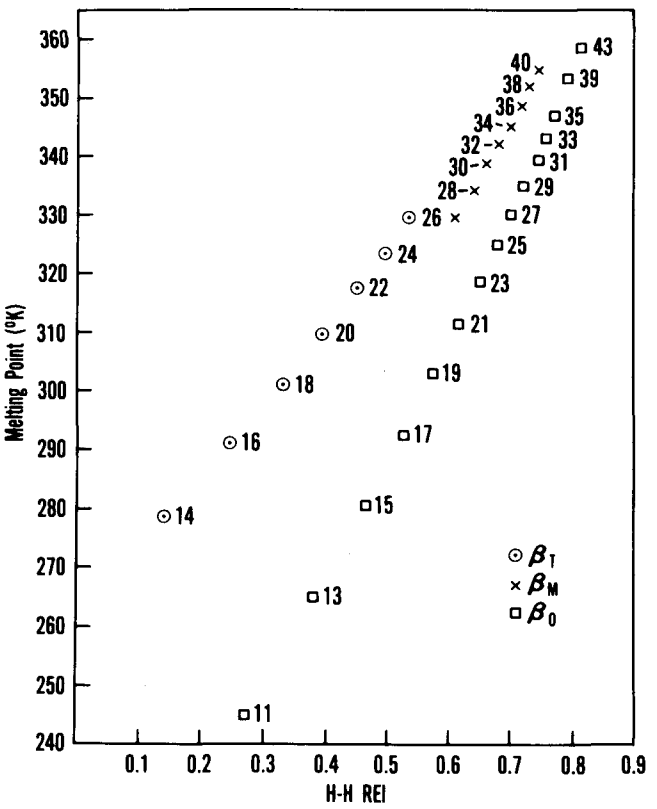

FIG. 3. Computer H-H REI (ratio of estimated interactions) results vs. melting point for n-alkanes.

TABLE IV

Middle of Chain H-H Contribution for Subcell Packings in Alkanes

Hydrocarbon chain length	REI X 100 (%)			
	H	β_T	β_O	β_M
10	21.6	---		---
11	29.2		27.1	
12	35.5	---		16.4
13	40.7		38.2	
14	45.2	14.0		28.1
15	49.0		46.4	
16	52.4	24.6		37.0
17	55.3		52.7	
18	57.9	32.9		43.9
19	60.2		57.7	
20	62.3	39.5		49.5
21	64.1		61.7	
22	65.8	45.0		54.0
23	67.3		65.0	
24	68.7	49.5		57.8
25	70.0		67.8	
26	71.2	53.4		61.0
27	72.3		70.2	
28	73.3	56.7		63.8

stable for odd alkanes shorter than C_{20}-C_{22} but unstable for the shorter even-length alkanes (6). REIs for α_H subcell packing, which increase in magnitude with increasing chain length, exceed 60% at C_{20} and C_{22}; values for these two chain lengths are 62% and 66%, respectively (Table IV). A particular crystal form would thus seem to be stable if the middle of the chain contributes more than 60% of the molecule's stabilizing interaction energy. Such reasoning alone, however, does not explain why odd alkanes below C_{20}-C_{22} have stable α_H forms while even alkanes do not.

Chains that differ by only one -CH_2- group should show almost equivalent stability in the α_H form because their vertical orientation with respect to the end group planes diminishes possible differences in end group effects. The REIs for odd α_H alkanes are about the same as those for β_O (Table IV), which is consistent with the fact that both forms are stable structures for odd alkanes (6). There is little internal driving force to change the α_H to β_O. Further transition from α_H or β_O forms can occur if favored energetically, but the end group asymmetry inherent in odd chain structures makes it likely that odd and even alkanes will follow dissimilar paths. This is particularly so with the short alkanes in which end group interactions contribute a more significant effect.

In tilted configurations, if an odd alkane assumes a low-energy conformation at one end, the other end of the zig-zag chain must adopt a different presumably higher energy position (6). Even chains, however, possess symmetry conducive to the same stabilizing interactions at both ends of the molecule (6). Accordingly, large differences were found between α_H and β_T for even alkanes (Table IV), especially in the 14-20 chain length region, where end group effect predominates in favor of the β_T form. It is thus hardly surprising that α_H is a transient form for short chain even alkanes. The energetic advantage conferred by large end group effect provides substantial inducement for such alkanes to assume the low energy β_T form. At C_{22}, however, the end group effect of β_T drops below 60%, while the REI of α_H is above 60%.

Solid Phase Behavior

Transformations and stabilities discussed in earlier sections and the known melting behavior of n-alkanes are summarized in Figure 4. On cooling from the melt, C_{20}

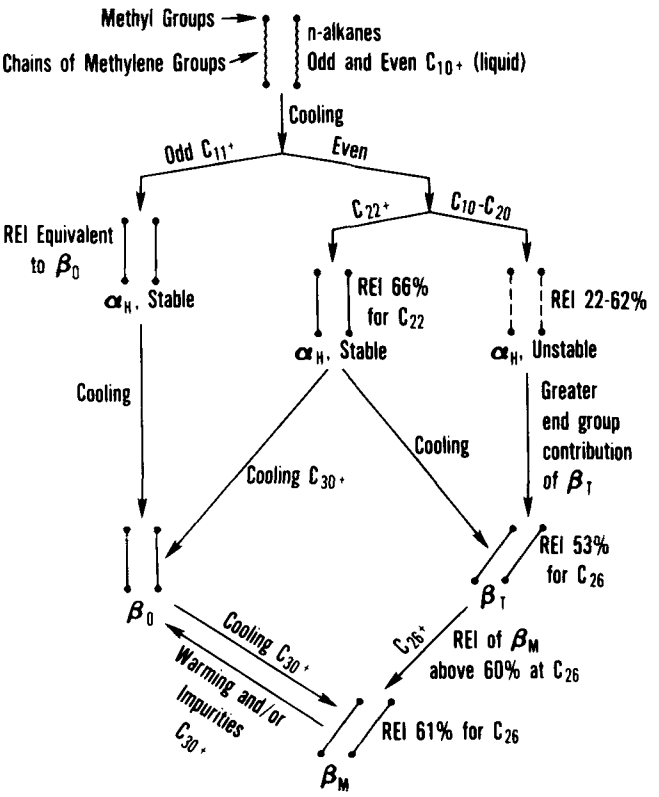

FIG. 4. Chain length dependent phase behavior of odd and even n-alkanes.

and shorter even alkanes pass through an unstable α_H form to a stable β_T form, while those longer than C_{20} remain in a stable α_H form until further cooling transforms them to β_T. Above C_{26}, where the REI is greater than 60%, the even alkanes change to β_M. Even alkanes above C_{30} do not ordinarily pass through β_T on cooling from α_H but change to β_O and finally to β_M (6). The odd alkanes above C_{11}, however, all assume a stable α_H structure and on further cooling, the β_O form.

Transitions involving chain lengths greater than C_{26} have not been discussed in terms of the computer results, because their reported behavior is more dependent on experimental conditions and purity of sample. Overall, the energy in end group packing is most important in determining structure. At an REI of 0.5, i.e., equal mid-chain and end group participation, structures prone to change should produce about equal amounts of the two forms. Instead, one form persists and the change does not occur until the REI exceeds 0.6. Equivalent interactions need not be distributed equally. From Table II, interaction energies in β_M from "CH_3 protons" to "middle-of-chain" are approximately of the same order, while the "CH_3 protons" energy of β_T is considerably higher than that of the other carbon positions. The energy of the end-group contribution for β_T is concentrated at the methyl gap and could be considered a relatively strong noncovalent bond. It is tempting to speculate that more middle-of-chain energy is needed to disrupt this single stronger center of energy than is needed to break apart many weaker centers spread over a larger area.

Polyethylene

Results using H-H REI were very similar to those from C-H, C-C, and total REI (Table III). Accordingly, plots and resulting conclusions using the total REI values vs. melting points would be essentially the same as those based on the individual interactions. Because the standard errors were

quite low for the parabolic lines of Figure 3, the following equations can be used to calculate accurately the melting points in the n-alkanes.

$$\beta_T \text{ (K)} = 45.72\ REI^2 + 98.33\ REI + 263.88$$

$$\beta_O \text{ (K)} = 95.13\ REI^2 + 104.17\ REI + 210.75$$

$$\beta_M \text{ (K)} = 143.11\ REI^2 - 9.86\ REI + 282.19$$

In these series of alkanes, the EI contribution for methyl protons and protons on carbons to the middle-of-chain will remain constant. As chain lengths increase, the middle-of-chain contribution will increase with a corresponding decrease in the percent of CH_3 contribution, until in polyethylene the end-group effect will become negligible and REI in the above equations will approach 1.0. Therefore, the relationship should predict the melting point of the infinitely long hydrocarbon chain of polyethylene. Polymer chains are thought to be oriented normal or very nearly normal to the plane of the crystal layers (14). Since Bunn (3) has reported the subcell of polyethylene to be orthorhombic, the limiting melting point predicted from the β_O equation is 137 C. The highest melting point observed for linear polyethylene for high molecular weight is 138.5 C (12). Niegisch and Swan (13) have suggested that the Bunn cell of polyethylene is really only a subcell; the real cell is triclinic. If the overall structure is triclinic, then chains must be somewhat tilted with respect to the end-group layers and the β_M equation becomes more applicable. The limiting melting point predicted is 142.4 C. Using the r^2 data of β_M, the prediction changes only to a value of 142.6 C. Although the folded chain structure of polyethylene (14) was not considered in the calculations, these values are in good agreement with the 145.5 C value predicted by Flory and Vrij (13) as the limiting melting point of the orthorhombic crystalline form in the n-paraffin hydrocarbon series. Their procedure involved the plotting of a function involving the enthalpy of fusion and heat capacity of polyethylene vs. the temperature difference between each particular n-hydrocarbon melting point and an assumed value for the polyethylene melting point. However, the enthalpy of fusion and heat capacity are not well established for polyethylene, and the limiting melting point is subject to the values chosen. Our prediction is based merely on the geometry of the crystalline forms, the recorded melting points of n-alkanes, and an interatomic interaction function which does not have to correspond to classical procedures.

ACKNOWLEDGMENTS

The authors thank G.F. Spencer and J.O. Ernst for assistance in computer programming and T.D. Simpson and M.A. Taylor for helpful discussion.

REFERENCES

1. Hagemann, J.W., W.H. Tallent, and K.E. Kolb, JAOCS 49:118 (1972).
2. Larsson, K., Ark. Kemi 23:35 (1965).
3. Bunn, C.W., Trans. Faraday Soc. 35:482 (1939).
4. Larson, K., Ark. Kemi 23:1 (1965).
5. Brodhurst, M.G., J. Res. Natl. Bur. Stand. A66:241 (1962).
6. Turner, W.R., Ind. Eng. Chem., Prod. Res. Dev. 10:238 (1971).
7. Hine, J., "Physical Organic Chemistry," McGraw-Hill Book Company, Inc., Second Edition, 1962.
8. Coiro, V.M., E. Giglio, A. Lucano, and R. Puliti, Acta Crystallogr. B29:1404 (1973).
9. Larsson, K., JAOCS 43:599 (1966).
10. Lennard-Jones, J.E., Proc. Phys. Soc. London 43:461 (1931).
11. Mazee, W.M., Rec. Trav. Chim. 67:197 (1948).
12. Parks, G.S., G.E. Moore, M.L. Renquist, B.F. Naylor, L.A. McClaine, P.S. Fujii, and J.A. Hatton, J. Am. Chem. Soc. 71:3386 (1949).
13. Flory, P.J., and A. Vrij, Ibid. 85:3548 (1963).
14. Billmeyer, Jr., F.W., "Textbook of Polymer Science," John Wiley and Sons, Inc., 1966.
15. Chiang, R., and P.J. Flory, J. Am. Chem. Soc. 83:2857 (1961).
16. Niegisch, W.D., and P.R. Swan, J. Appl. Phys. 31:1906 (1960).

[Received July 19, 1979]